



Massive Stars in the SDSS-IV/APOGEE-2 Survey. II. OB-stars in the W345 Complexes

Alexandre Roman-Lopes^{1,2,3} , Carlos G. Román-Zúñiga² , Mauricio Tapia² , Jesús Hernández², Valeria Ramírez-Preciado² , Guy S. Stringfellow⁴ , Jason E. Ybarra⁵ , Jinyoung Serena Kim⁶ , Dante Minniti^{7,8,9} , Kevin R. Covey¹⁰ , Marina Kounkel¹⁰ , Genaro Suárez² , Jura Borissova^{8,11} , D. A. García-Hernández^{12,13} , Olga Zamora¹³, and Juan David Trujillo¹⁴

¹ Department of Physics & Astronomy—Universidad de La Serena—Av. Juan Cisternas, 1200 North, La Serena, Chile; aroman@userena.cl

² Instituto de Astronomía, UNAM, Unidad Académica en Ensenada, Ensenada 22860, Mexico

³ Programa de Estancias de Investigación DGAPA UNAM, Mexico

⁴ Center for Astrophysics and Space Astronomy, Department of Astrophysical and Planetary Sciences, University of Colorado, 389 UCB, Boulder, CO 80309-0389, USA

⁵ Department of Physics, Bridgewater College, Bridgewater, VA 22801, USA

⁶ Steward Observatory, University of Arizona 933 N. Cherry Avenue, Tucson, AZ 85721-0065, USA

⁷ Departamento de Ciencias Físicas, Facultad de Ciencias Exactas, Universidad Andres Bello, Av. Fernandez Concha 700, Las Condes, Santiago, Chile

⁸ Millennium Institute of Astrophysics, Av. Vicuna Mackenna 4860, 782-0436, Santiago, Chile

⁹ Vatican Observatory, V00120 Vatican City State, Italy

¹⁰ Department of Physics & Astronomy, Western Washington University, 516 High Street, Bellingham, WA 98225-9164, USA

¹¹ Instituto de Física y Astronomía, Universidad de Valparaíso, Av. Gran Bretaña 1111, Playa Ancha, Casilla 5030, Chile

¹² Instituto de Astrofísica de Canarias, E-38205 La Laguna, Tenerife, Spain

¹³ Departamento de Astrofísica, Universidad de La Laguna (ULL), E-38206 La Laguna, Tenerife, Spain

¹⁴ Department of Astronomy, University of Washington, Box 351580, Seattle, WA 98195, USA

Received 2018 December 2; revised 2019 January 4; accepted 2019 January 27; published 2019 March 5

Abstract

In this work, we have applied a semi-empirical spectral classification method for OB-stars using the APOGEE spectrograph to a sample of candidates in the W3–W4–W5 (W345) complexes. These massive star-forming regions span over 200 pc across the Perseus arm and have a notorious population of massive stars, from which a large fraction are members of various embedded and young open clusters. From 288 APOGEE spectra showing *H*-band spectral features typical of O- and B-type sources, 46 probably correspond to previously unknown O-type stars. Therefore, we confirm that Br11–Br13 together with He II $\lambda 16923$ (7–12) and He II $\lambda 15723$ (7–13) lines contained in the APOGEE spectral bands are useful in providing spectral classification down to one spectral subclass for massive stars in regions as distant as $d \approx 2$ kpc. The large number of newly found O-type stars as well as the numerous intermediate-mass population confirm that W345 is a very efficient massive star factory, with an integral stellar population probably amounting several thousand solar masses.

Key words: Galaxy: stellar content – infrared: stars – stars: early-type – stars: massive – techniques: spectroscopic

Supporting material: figure set, machine-readable tables

1. Introduction

The W3–W4–W5 region (hereafter, W345) is one of the closest massive ($\geq 10^5 M_\odot$) star-forming complexes. Its location right at the Galactic plane on the Auriga region of the Perseus arm, at a relatively close distance ($d \approx 2$ kpc Hachisuka et al. 2006), and its morphology, almost perpendicular with respect to the line of sight, makes it an archetypal massive star nursery. It has been the subject of numerous studies dedicated to the characterization of young star cluster populations (Carpenter et al. 2000; Koenig et al. 2008; Deharveng et al. 2012; Chavarría et al. 2014; Kiminki et al. 2015; Román-Zúñiga et al. 2015; Jose et al. 2016; Panwar et al. 2017; Sung et al. 2017) and the effects of the local environment on young cluster evolution (Rivera-Ingraham et al. 2011, 2013, 2015; Román-Zúñiga et al. 2015). The complex contains three main ionization regions. The easternmost region, W5, is associated with the young open cluster IC 1848, while the largest central region, W4, is associated with the young open cluster IC 1805. At the western edge of the complex lies the W3 region, in a massive molecular gas ridge hosting a family of embedded clusters (Thronson et al. 1985).

In this sense, it is clear that the massive star populations in W345 are crucial for the evolution of the complex. They are

responsible for the expansion of the large H II regions that shape their morphology, currently providing much of the mechanical energy that is rapidly dispersing the molecular gas of the cloud (Rivera-Ingraham et al. 2013; Román-Zúñiga et al. 2015). Previous studies on W345 indicate that several stellar groups are probably in different evolutionary stages. Bik et al. (2012) suggest that W3-Main harbors several H II regions, ranging from very young hyper-compact H II regions (HCH—few 10^3 yr old) and ultra-compact H II regions (UCH—about 10^5 yr old) to more evolved, diffuse H II regions with ages of a few 10^6 yr (Wood & Churchwell 1989). The massive stars in IC 1805 have been characterized (e.g., Rauw & De Becker 2004; De Becker et al. 2006; Rauw & Nazé 2016), along with multi-wavelength studies of the low and intermediate-mass population (e.g., Straizys et al. 2013; Panwar et al. 2017) and of the physics of the W4 super-bubble expansion (e.g., Basu et al. 1999; Gao et al. 2015). For the W5 complex, studies like those of Karr & Martin (2003) and Niwa et al. (2009) discuss the expansion of the H II regions and the effects on cluster evolution. Along the same line, Navarete et al. (2011) concluded that there is a mixing of evolutionary stages across the W3 complex, as indicated by their classification of the OB stars. In order to uncover the formation and early evolution processes of this star-forming complex, it is paramount to study

in great detail the evolution of young H II regions, and in particular, the associated O- and early-B stellar content as they are probably the main source of the ionizing photons.

This paper is the second of a series in which we describe our study of OB-stars using SDSS-IV/APOGEE-2 data (Roman-Lopes et al. 2018). It comes from an ancillary project aimed at studying the unknown O-star population dispersed along the W345 Galactic complex. These new APOGEE-2 data reveal a large number of new O stars. Our results confirm the reliability and efficiency of this instrument for identifying and investigating large populations of OB-stars, and are especially useful when studying highly obscured Galactic environments where optical spectroscopy is difficult.

In Section 2, we briefly describe the APOGEE-2 survey, and in Section 3, we present the W345 APOGEE-2 Ancillary project, as well as the results and discussion. Finally, in Section 4, we present our conclusions.

2. Hot Stars in SDSS-IV/APOGEE-2 Survey

The Apache Point Observatory (APO) Galactic Evolution Experiment (APOGEE) was conceived as one of the main core surveys of the third stage of the Sloan Digital Sky Survey (SDSS-III; Gunn et al. 2006; Eisenstein et al. 2011; Majewski et al. 2017). It aims to observe about 130,000 spectra of red giant stars in all Galactic components, providing valuable constraints for the study of the chemical history and evolution of the Galaxy. The second phase of the program, the APOGEE-2 Survey (Blanton et al. 2017), extends the data set to the Southern hemisphere from Las Campanas Observatory (LCO), performing a unique all-sky spectral database of more than 300,000 sources, including the partial coverage of high-extinction regions, toward the Galactic center, the Bulge, as well as the Magellanic Clouds (Zasowski et al. 2017).

The survey is made possible through the two APOGEE instruments: APOGEE-2N located at the APO, and APOGEE-2S located at the LCO (Wilson et al. 2010). Each of them is a 300-fiber spectrograph working in the wavelength range 15000 Å–17000 Å in the near-infrared (NIR) H -band. It works over three non-overlapping detectors that individually cover the ranges 15145–15810 Å (blue), 15860–16430 Å (green), and 16480–16950 Å (red), with a mean resolving power $R \sim 22500$. Each APOGEE-2 observation (or visit) is a 1-hr block integration covering fields of radius 1.5 and 1.0 for APOGEE-2N and APOGEE-2S, respectively. Not all of the 300 fibers are dedicated to science targets in each visit, as a fraction (about 35 fibers per visit) are dedicated to telluric and sky line correction. For further details regarding the APOGEE-2 data reduction procedure, see Nidever et al. (2015).

3. The W345 APOGEE-2 Ancillary Project

Because the W345 complex is an excellent site to study the formation and evolution of massive stars, it was chosen as a suitable target for an ancillary program of the SDSS-IV/APOGEE-2 Survey. It is aimed to study low- to high-mass young stars, extending the usage of the bleAPOGEE-2 spectrograph from nearby low-mass star-forming complexes with heliocentric distances smaller than 1 kpc (e.g., Cottaar et al. 2015; Foster et al. 2015; Da Rio et al. 2016; Kounkel et al. 2018), to more distant young stellar populations. As part of this program, dozens of O- and B-star candidates were observed with the APOGEE-2N spectrograph in W345. By

applying the methodology developed by Roman-Lopes et al. (2018, hereafter Paper I), we were able to identify and classify dozens of new massive stars in the W345 complex.

3.1. Candidate OB-stars: Selection Criteria

The candidate O- and B-stars included in this work were selected from the 2MASS Point Source Catalogue (Skrutskie et al. 2006) using a combination of NIR photometric and color selection criteria described in detail by Roman-Lopes et al. (2016). The derived primary catalog of OB star candidates was then cross-matched with the positions of known O- and B- stars, found in the SIMBAD¹⁵ and VIZIER¹⁶ databases. From the resulting O- and B-stars candidate sample, some sources resulted (as expected) to be already known OB-stars. For completeness, they were also included in the primary OB star sample.

The two fields of the W345 ancillary program (W34 and W5 —see Figure 1) are centered on the coordinates presented in Table 1. Due to the APOGEE-2 survey magnitude and signal-to-noise (S/N) constraints, in the case of the W345 ancillary project, only sources with H magnitudes in the range $7 < H < 13.0$ were observed. On the other hand, the number of targets that can be observed from a target sample in a given plate is limited, not only by the number of science fibers available, but also by the “fiber-collision issue”, which in turn is set by the physical size of the optical fiber connector. For APOGEE-2N, the effective collision limit is 72 arcsec. For this reason, when observing high-density regions like clusters, the solution is to dedicate more visits to a given field, each with a slightly distinct plate design, allowing one to observe a different group of sources. A fraction of the targets are repeated to allow one to reach the required S/N for the faintest sources (for example, an $H = 12.5$ source requires three 1-hr visits to achieve an S/N = 100). Finally, from the total number of available fibers in a given plate, not all were used to observe sources from the O- and B-star candidates sample, as the ancillary project also contemplates a number of fibers for the low- to intermediate-mass young stars.

For the W345 APOGEE-2 ancillary project, a total of 11 plates were used: 6 plates for W34 and 5 plates for W5 (Figure 1). For plates 9245 and 9249 (W3+W4), extra visits were awarded. The data were collected between fall 2016 and winter 2017. In Table 1, we present a summary of the observations with some key information of the W345 SDSS-IV/APOGEE-2 ancillary program, including plate information and the MJD of each visit.

3.2. O-stars in the W345 APOGEE-2 Ancillary Project

From the plates and epochs listed in Table 1, a total of 718 stars (from all type of targets, e.g., candidate and known O- and B-stars, low to intermediate young stars, etc.) were observed at least once. From the visual inspection of the line features present in the spectra of APOGEE-2 W345 sources (and accordingly with Paper I), we concluded that 288 spectra present features typical of O- or B-type stars (hereafter OB-type sample). The remaining sources compound a sample mostly formed by: (i) low- to intermediate-mass stars, (ii) A-type stars used for telluric correction purposes, and (iii) a number of sources

¹⁵ <http://simbad.u-strasbg.fr/simbad/>

¹⁶ <http://vizier.u-strasbg.fr/viz-bin/VizieR>

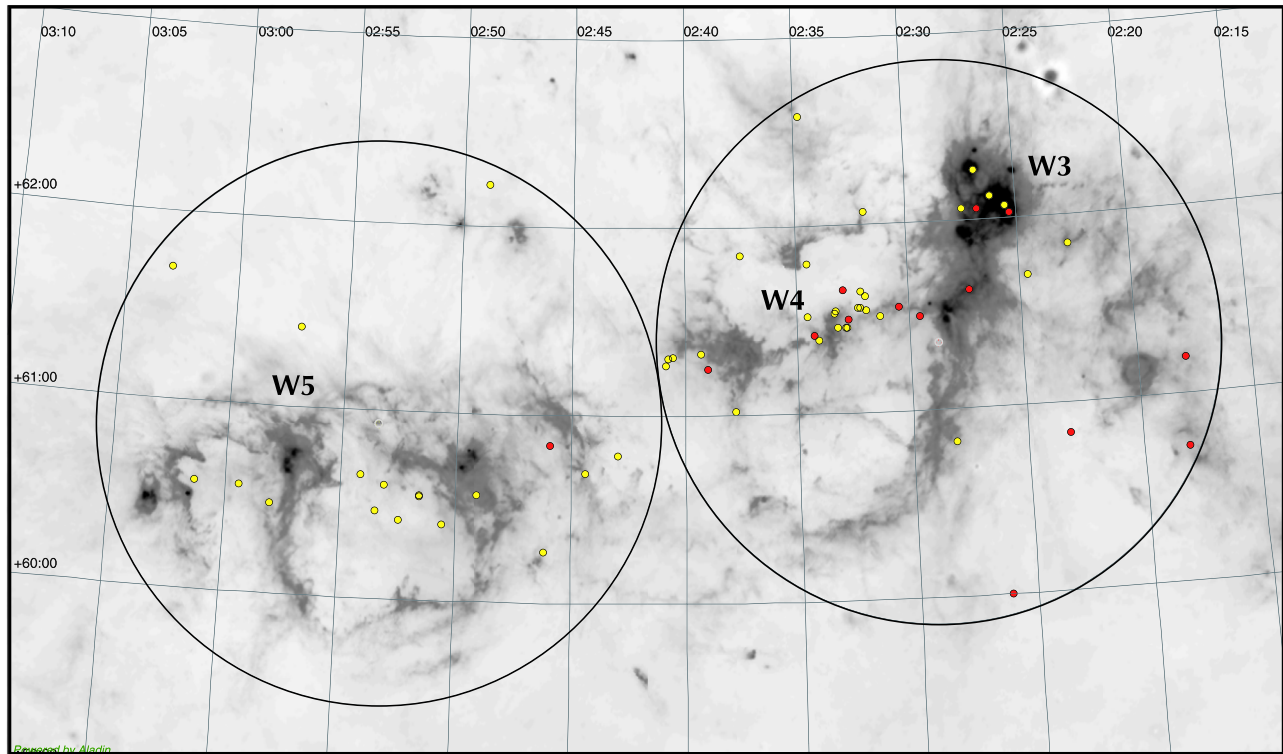


Figure 1. W345 APOGEE-2 OB star Sample position map. The background image shows dust emission from the WISE (<https://irsa.ipac.caltech.edu/applications/wise/>) WSSA 12 μm survey. The large circles show the extension of the two APOGEE-2 North fields for this project. The yellow filled symbols show the positions of the 60 O- and early-B stars classified in this work, with the red filled symbols showing the positions of known O-stars previously classified in the literature.

Table 1
Summary of the SDSS-IV/APOGEE-2 W345 Ancillary Program

Program	Plate Number	MJD	R.A.	Decl.
W3-4	9246	57650	37.1726	61.4056
W3-4	9247	57677	37.1726	61.4056
W3-4	9245	57710	37.1726	61.4056
W3-4	9248	57762	37.1726	61.4056
W3-4	9245	57764	37.1726	61.4056
W3-4	9249	57766	37.1726	61.4056
W5	9251	58007	43.3700	60.8982
W3-4	9249	58008	37.1726	61.4056
W5	9252	58008	43.3700	60.8982
W5	9253	58009	43.3700	60.8982
W5	9255	58029	43.3700	60.8982
W3-4	9250	58037	37.1726	61.4056
W5	9256	58039	43.3700	60.8982

showing spectral features typical of cool stars (e.g., giants and dwarfs) of the Galactic disk population, probably not related to the W345 complex. A detailed analysis and statistics of the number of sources of each type that resulted to be observed in the W345 APOGEE-2 ancillary project is beyond the scope of this paper. Such analysis will be part of an upcoming paper dedicated to present the target selection methodology and cadence for the entire sample of the W345 APOGEE-2 ancillary project (A. Roman-Lopes et al. 2019, in preparation).

For each star of the OB-type sample, we carefully measured the associated spectral line profile parameters using the routines available in the IRAF¹⁷ SPLLOT package. We performed model

fittings using both Voigt and single-Gaussian profiles, with an associated continuum determined from regions far from the observed line wings. The uncertainties in the equivalent widths (EWs), and full width half maximum (FWHM) values range from about 10% in those spectra with the highest S/N (usually above 250–400), to about 20% for those spectra presenting lower S/N values (typically in the range 100–150).

In addition to the EW, and FWHM values mentioned above, we performed radial velocity measurements from the Doppler shifts in the corresponding APOGEE-2 spectral lines. This was done for all stars listed in Table 2. However, we point out that a detailed kinematic analysis and other physical aspects related to the entire OB-type sample, is outside of the scope of this work and will be presented in future articles of this series.

3.2.1. O-star List and Spectral Line Parameters

Based on the presence or absence of the He II 7–12 and He II 7–13 lines, and/or the Brackett line parameter criteria $\text{EW}[\text{Br}11] < 2.0 \text{ \AA}$ and $\text{EW}[\text{Br}13] < 1.5 \text{ \AA}$, together with the semi-empirical classification criteria defined in Paper I, 46 of 60 sources (about 77%) are classified as mid- to late-type O stars, with the remaining presenting hydrogen Brackett EW line parameters typical of late-O/early-B (O9-B1) type stars (Roman-Lopes et al. 2018).

Figure 2 and its full version online, show the relevant sections of the APOGEE-2 spectral windows that contain the main features of interest for estimating the spectral types and luminosity classes: (a) the hydrogen lines of the Brackett series $\lambda 16811$ (11–4), $\lambda 16113$ (13–4), and (b) two He II lines, $\lambda 15723$ (7–13) and $\lambda 16923$ (7–12). They vanish in the case of dwarfs of spectral types later than O8.5, and for spectral types

¹⁷ <http://iraf.noao.edu/>

Table 2
SDSS-IV/APOGEE-2 Survey of OB-stars in W345

Star	APOGEE-2 ID	ID (Literature)	<i>H</i> mag (2MASS)	SpType	Lum. Class	Qual.	References ^a
1	2M02315709+6136440	BD+60 497	7.42	O6.5 + O8-B0	v	...	(5)
2	2M02264527+6203075	[OWK2005] 3041	7.68	O9.7	I	a	(4)
3	2M02280909+6049108	...	8.98
4	2M02541067+6039036	BD +60 586	7.71	O7	v	z	(5)
5	2M02293046+6129440	LS I +61 270	8.64	B0	III	...	(10)
6	2M02340253+6123108	BD+60513	8.16	O7	v	z	(1)
7	2M02252738+6203432	[BEC76] W3 j	10.45	B0-B2	v	...	(11)
8	2M02321675+6133149	BD +60 499	9.00	O9.5	v	...	(5)
9	2M02461010+6015576	...	10.17	(2)

Note.

^a List of OB stars observed in the W345 complexes with APOGEE-2. Column (1) contains the internal ID; column 2 the APOGEE-2 ID; column 3 the source ID found in the literature; column 4 the 2MASS *H*-band magnitudes; column 5 the spectral type taken from the literature; column 6 the corresponding luminosity class; column 7 the associated qualifier; and column 8 the reference from which the spectral types and luminosity classes were taken. References: (1) Maíz Apellániz et al. (2016) (2) Hiltner (1956) (3) Sota et al. (2014) (4) Mathys (1989) (5) Sota et al. (2011) (6) Voroshilov et al. (1985) (7) Massey et al. (1995) (8) Abt & Corbally (2000) (9) Oey et al. (2005) (10) Shi & Hu (1999) (11) Cohen & Lewis (1978) (12) Kiminki et al. (2015) (13) Hardorp et al. (1959) (14) Rydstrom (1978). Table 2 is published in its entirety in the machine-readable format. A portion is shown here for guidance regarding its form and content.

(This table is available in its entirety in machine-readable form.)

O9-O9.5 in the case of super-giants. As shown by Roman-Lopes et al. (2018), the relative intensities of the He II lines, as well as the Brackett line strength, change from the later to the earliest O-types, with the hydrogen and helium lines presenting (in general) much broader line profiles in class V O-stars, than in those of class I–II.

3.2.2. Luminosity Classes and Spectral Types Based on the APOGEE-2 Line Parameter Measurements

APOGEE-2 spectra of O-stars (dwarf and sub-giants) of spectral types earlier than O9 in general present the 7–12 and/or the 7–13 He II lines (however not in all cases) (Roman-Lopes et al. 2018). In Paper I, we concluded that the EW values of the Br11 and Br13 hydrogen lines together with those for the two He II lines (when available) enable reliable spectral type estimates using linear relations, which can be chosen based on an EW[Br11+Br13] versus mean FWHM[Br11–Br13] diagram, like the one presented in Figure 3. There, the O-star locus for luminosity classes I–II–III is delimited by the red dotted lines, with the O-star locus for classes IV–V indicated by the blue solid lines. For completeness, in the same diagram, we also indicate the B-stars loci, for classes I–II–III (yellow lines) and IV–V (green lines). Notice that we have omitted from this plot all B-type stars in the W345 OB sample, e.g., those that do not fit the EW criteria for O- and/or late-O to B0-B1 stars defined in the previous section (Roman-Lopes et al. 2018). We see in this diagram that the majority of the O-stars in the W345 APOGEE-2 sample probably belong to luminosity classes IV–V. The O-type stars in Figure 3 are separated into two groups: the first group, represented by the blue filled circles, is composed exclusively of stars whose spectra present hydrogen Brackett line EWs satisfying the criteria $EW(\text{Br}11) < 1.0 \text{ \AA}$ and $EW(\text{Br}13) < 0.75 \text{ \AA}$ —“O-stars only”—Roman-Lopes et al. (2018). We notice that in the case of the earliest O-type stars, the measured Br13 EW values sometimes appear larger than the mentioned limits. Nevertheless, it is possible to discriminate early O-type stars from the mentioned B-type ones based also on the presence of the He II 7–12 and 7–13 line transitions. The second group (“[O + B0-B1] cand”), represented by the red filled squares, is composed by stars with EW measured

values in the range $1.0 < EW(\text{Br}11) < 2.1 \text{ \AA}$, and $0.75 < EW(\text{Br}13) < 1.5 \text{ \AA}$. These sources likely have spectral types in the ranges O7–O8 to B0–B1 (for additional details, see discussion in Roman-Lopes et al. 2018).

From the estimates of the luminosity classes (listed in Table 3), we derived spectral types using the hydrogen and helium EW values, and the relations derived in Paper I, which are listed as follow:

For early-B-type stars:

(a) Giants and super-giants (B0–B3)

$$\text{SpType} = 0.56 \times \text{EW}[\text{Br}11 + \text{Br}13] + 8.99 \quad (1)$$

(b) sub-giants and dwarfs (B0–B5)

$$\text{SpType} = 0.64 \times \text{EW}[\text{Br}11 + \text{Br}13] + 8.47 \quad (2)$$

with the numerical results from this equations related to the spectral types by 10 = B0, 11 = B1, ..., 15 = B5 (Paper I).

For O-type stars:

(a) Dwarfs and sub-giants

$$\text{SpType} [\text{He II } (7-12)] = -5.05 \times \text{EW}[7-12] + 9.32 \quad (3)$$

$$\text{SpType} [\text{He II } (7-13)] = -6.40 \times \text{EW}[7-13] + 9.10. \quad (4)$$

(b) Giants and super-giants

$$\text{SpType} [\text{He II } (7-12)] = -3.50 \times \text{EW}[7-12] + 9.59 \quad (5)$$

$$\text{SpType} [\text{He II } (7-13)] = -3.63 \times \text{EW}[7-13] + 9.48. \quad (6)$$

Likewise, the value 5 corresponds to O5, 6 to O6, ..., 9 to O9, 10 to B0.

Following Paper I, the criterion used to transform the numerical values into spectral types in the canonical way (e.g., O7.5, O9, B0.5, etc.), is to associate the values from Equations (1)–(6) to the corresponding intervals in the following sequences: For O-stars [(5.0–5.5), (5.5–6.0), ..., (9.0–9.5)] correspond to [(O5–O5.5), (O5.5–O6), ..., (O9–O9.5)], and for B-stars [(10–10.5), (10.5–11), ..., (14.5–15)] correspond to [(B0–B0.5), (B0.5–B1), ..., (B4.5–B5)]. In the case of stars with helium lines, the adopted spectral type is taken from the average value from the two lines (if available). On the other hand, for those sources without any helium absorption lines, we only assign lower and upper limits to the

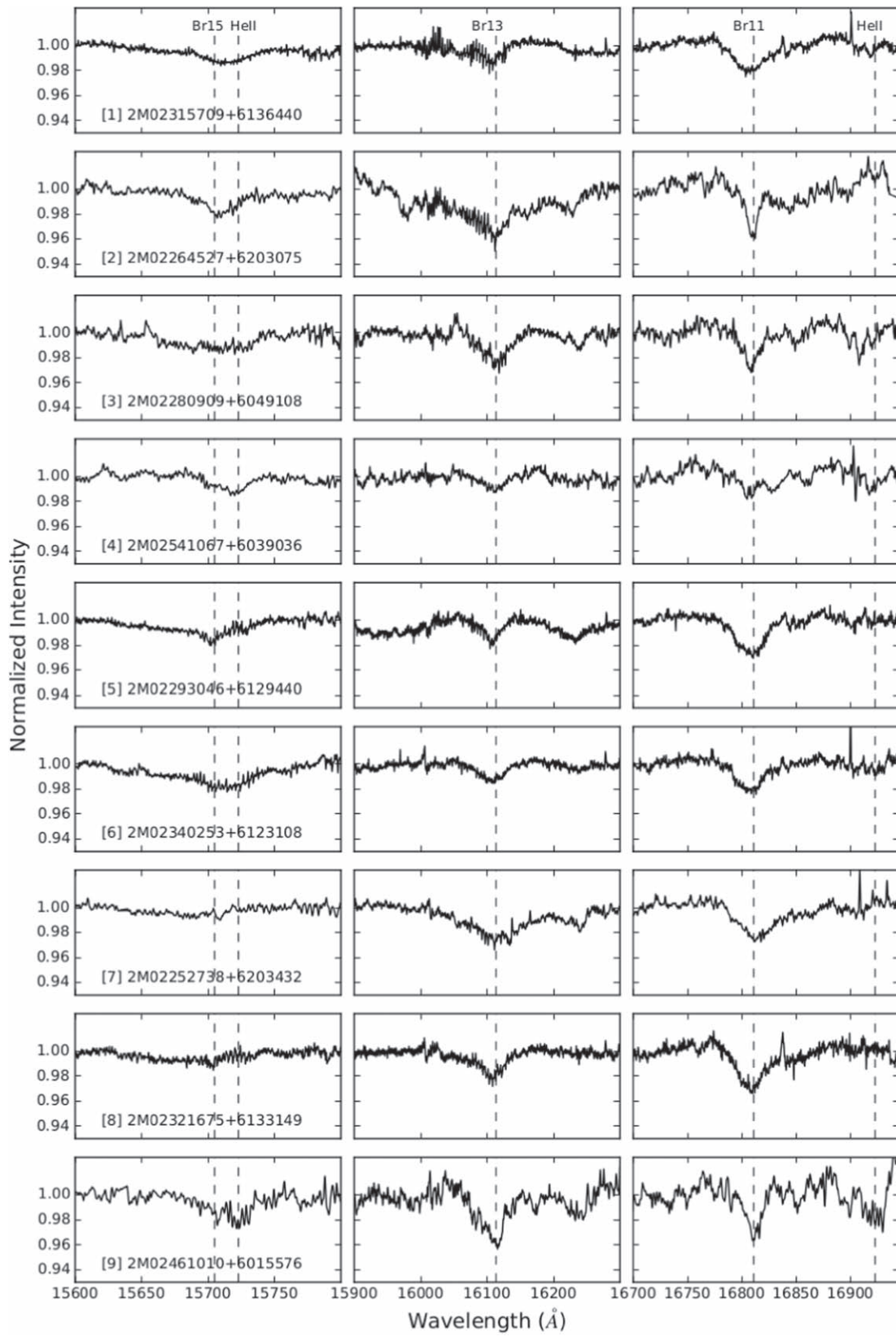


Figure 2. APOGEE-2 spectra of O-stars observed in the W345 complex. We show the APOGEE-2 spectral regions that include the main spectroscopic features (Br11 and Br13 hydrogen recombination lines plus the 7–12 and 7–13 Helium lines) used for spectral characterization. Only a sub-group of nine spectra (among the 60 O-stars selected by us) are shown here. The numbers between brackets correspond to the internal ID of the sources.

(The complete figure set (7 images) is available.)

Table 3
Line Parameters for OB-stars in W345^a

#	EW(A)	FWHM(A)	EW(A)	FWHM(A)	EW(A)	FWHM(A)	EW(A)	FWHM(A)	SpType	Lum. Class	SpType
	[Br11]	[Br11]	[Br13]	[Br13]	[He II 7–12]	[He II 7–12]	[He II 7–13]	[He II 7–13]	[This work]		[Literature]
1	0.72	31.72	0.42	33.96	0.09	8.10	0.35	24.59	O8.5-O9	IV–V	O6.5 + O8/B0
2	0.52	13.35	0.38	41.7	O9-O9.5	I-II	O9.7
3	0.52	16.9	1.01	42.49	0.45	22.99	0.55	30.40	O7.5	IV–V	...
4	0.54	28.34	0.47	39.14	0.65	22.20	0.43	13.71	O7	IV–V	O7
5	0.84	28.36	0.21	17.59	O9.5	I-III	O9.5
6	0.63	27.31	0.53	38.61	0.56	42.20	0.17	19.00	O7-O8	IV–V	O7
7	0.98	33.95	0.98	33.95	O9.5	IV–V	B0-B2
8	0.87	27.13	0.95	48.26	O9.5	IV–V	O9.5
9	0.68	17.2	1.33	38.21	O8.5	IV–V	...

Note.

^a Equivalent width and full width half maximum measurements for the the H I (Br11 and Br13) and He II (7–12 and 7–13) spectral lines detected in the spectra of the W345 APOGEE-2 O-star sample. Associated uncertainties on the quoted values are estimated to vary from 10% to 15%.

(This table is available in its entirety in machine-readable form.)

spectral type. However, in cases in which both results are similar, only the resulting spectral type (not a range) is assigned.

For example, APOGEE-2 W345 source #2 ([OWK2005] 3041) is a known O9.7 Ia star (Mathys 1989). It shows an unusually broad Br13 line, but from the observed Br11 line profile (and associated EW value of 13.4 Å), we assigned it class I–II, and accordingly, Equation (1) was applied. At the same time, lower limits for its spectral type were derived using Equations (5) and (6) in view of having $EW = 0$ for the helium lines. Considering the three possibilities, we derive the following O-sub-types for this star: 9.5 (from Br11+Br13), 9.1 (from He II 7–12), and 9.5 (from He II 7–13). Therefore, the final assigned classification was O9–O9.5 I–II, which is in good agreement with the spectral type and luminosity class reported in the literature from optical spectra for this star. A similar procedure was followed for all sources in the late-O/B0–B1 type group.

In Table 3, we list the sources classified accordingly with the procedure described above, along with their corresponding identifications (IDs) from the literature (when available). For each source, we also include the APOGEE-2 survey ID, the associate 2MASS *H*-band magnitudes and, when available, the spectral type and corresponding reference from the literature. Table 3 also lists the values of the measured line profile parameters. Out of 31 O-type stars previously classified in the literature as early- to mid-B-type stars, 27 are now classified as O6.5 to O9.5, and 4 as O9-B1 type stars. On the other hand, about 15 APOGEE-2 sources having no previous spectral classification have now received spectral types in the range O6.5 to O9.5. Finally, the remaining stars (14 sources) are compounded by known mid- to late-O stars spread across the W345 complex (see Figure 1).

Another example of estimated spectral type is that of source #13 in which both values derived from the EW of the hydrogen lines result O9.5 (considering an uncertainty of one sub-type). For comparison, we list in column 12 of Table 3 the spectral types from the literature. The agreement between our results and the spectral types from known stars in the literature is quite good (within one sub-class), with a few exceptions, in which the O-stars are members of binary

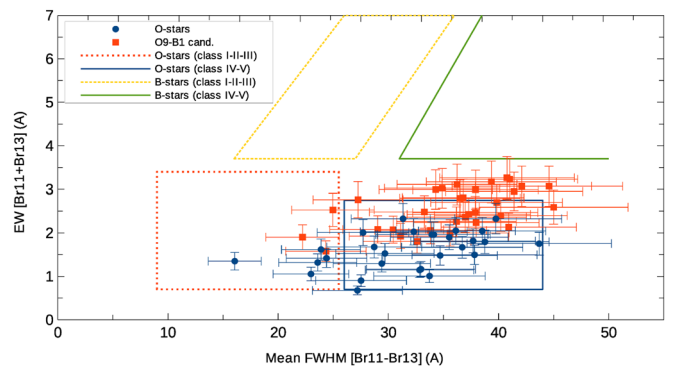


Figure 3. EW[Br11+Br13] vs. mean FWHM[Br11+Br13] diagram made from data in Table 3. (red dotted) O-stars of classes I–III. (blue solid line) O-stars of classes IV–V. (Green solid line) B-stars of classes IV–V. (Yellow dotted line) B-stars of classes I–III. The O-type stars are separated into two groups: The first, represented by the blue filled circles, is composed exclusively by stars whose spectra present hydrogen Bracket line equivalent widths satisfying the criteria $EW(\text{Br}11) < 1.0 \text{ \AA}$ and $EW(\text{Br}13) < 0.75 \text{ \AA}$ —“O-stars only”—Roman-Lopes et al. (2018). The second group—“[O + B0-B1] cand”, represented by the red filled squares, is composed of stars with EW measured values in the range $1.0 < EW(\text{Br}11) < 2.1 \text{ \AA}$, and $0.75 < EW(\text{Br}13) < 1.5 \text{ \AA}$. These sources likely have spectral types in the range O9 to B0-B1. For additional details, see discussion in Roman-Lopes et al. (2018).

systems. Interestingly, in such cases the results from APOGEE-2 spectra apparently tend to point to the later-type components.

3.3. Optical Spectra for Eight Stars in the W345 APOGEE-2 O-star Sample

Considering that the MK spectral classification system for OB-type stars is based on optical spectra, in order to further test our NIR-based classification results, we obtained new medium-resolution optical spectra for a number of stars in the W345 APOGEE-2 O-star sample, and used them to derive optical spectral classifications:

Optical spectra for sources #3, #13, #17, #21, #25, #26, #20, and #46 were obtained with the 2.12 m Telescope at the Observatorio Astronómico Nacional at Sierra San Pedro Mártir in Baja California, México. We used the Echelle spectrograph and the Marconi-4 2048 × 2048 CCD camera.

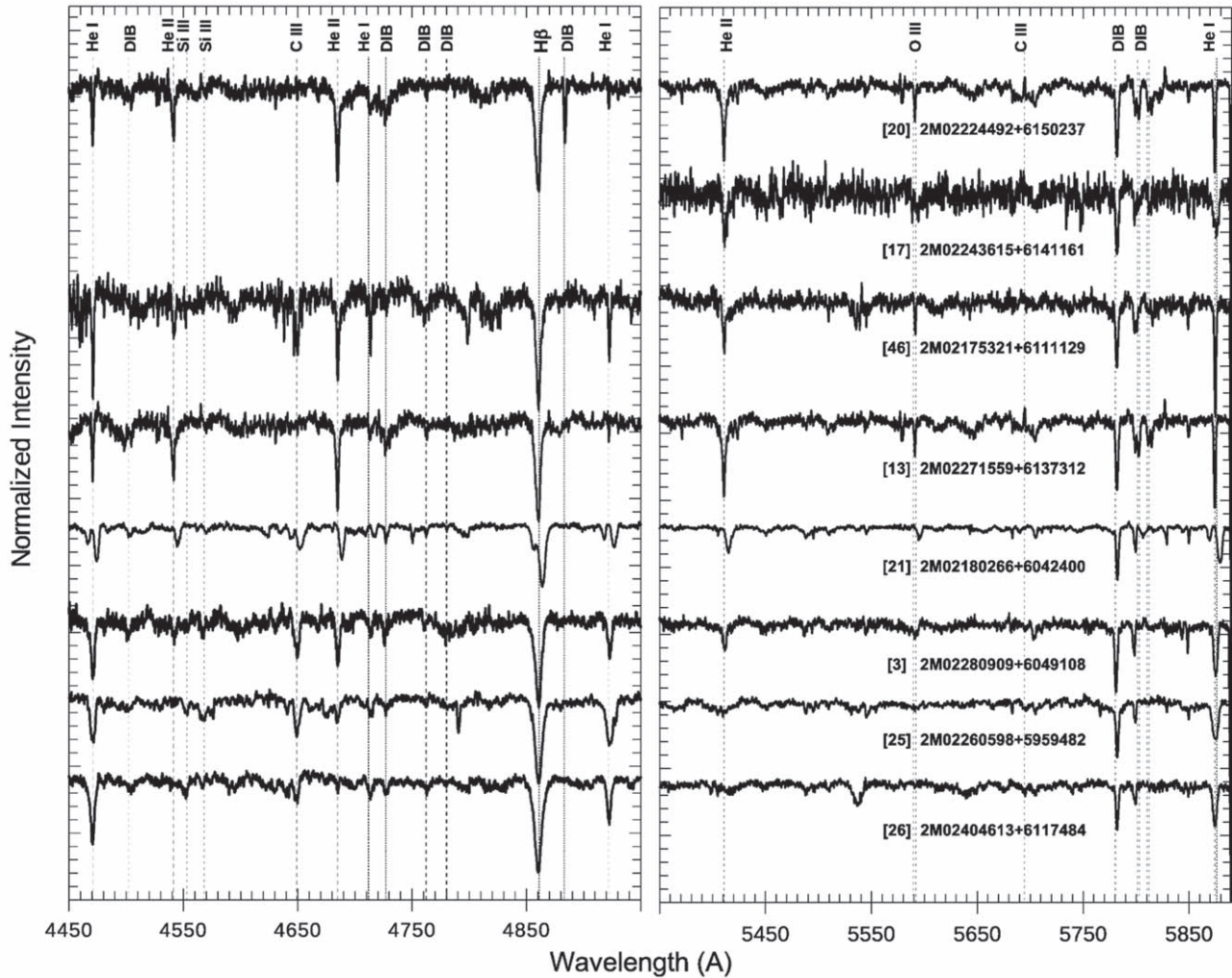


Figure 4. Optical medium-resolution spectra for eight stars in our sample. From careful examination of the blue and red spectrograms of source #21, one can see that all He I lines are double, indicating that the star is a binary system. Indeed, the He II $\lambda 4542$ and He II $\lambda 5411$ lines of the primary are much stronger than those from the secondary (blueshifted). On the other hand, the He I $\lambda 4471$ and He I $\lambda 5876$ lines seem to be much stronger compared with the associated He II $\lambda 4542$ and He II $\lambda 5411$ lines (blueshifted). Based on the observed line intensities and ratios, and using the criteria defined by Sota et al. (2011), we conclude that source #21 is probably composed of O8 III and O9.5 III stars (see discussion).

For these observations, we selected the $200 \mu\text{m}$ ($2''.75$) slit width, a cross-dispersing grating of $300 \text{ lines mm}^{-1}$ and a 3600 \AA cutoff filter, together with a $13''$ mask to separate contiguous orders. The resultant resolution was $R \approx 18000$ within orders 30–61, corresponding to the $3600 < \lambda / \text{\AA} < 7000$ range. Each observation in this program consisted of two to three sets of 1800 s exposures, preceded and followed by a 150 s ThArNe lamp exposure to allow for wavelength calibration.

These Echelle spectra were reduced using standard techniques through the use of the IRAF ONEDSPEC, TWODSPEC, and APEXTRACT packages. The one-dimensional spectra of the science targets were extracted from the two-dimensional frames by adding up pixels in the data range and subtracting off the background value for each order column, which was measured as the median of contiguous non-target pixels. Cosmic rays and other anomalous signal detection were suppressed from each of the extracted spectra by removing pixels that deviate 5σ or more from the mean within a 100 pixel wide box that steps through the spectrum. The bad pixels were replaced through linear interpolation on the removed data range, and the wavelength calibration was performed using the

ThArNe lamp spectra. The final optical Echelle spectra for the program stars were then normalized through the fitting of the continuum in the associated wavelength ranges.

3.4. Optical Spectra: Results and Discussion

In Figure 4, we present the normalized San Pedro Martir Echelle spectra in the ranges $4450\text{--}4950 \text{ \AA}$ and $5350\text{--}5890 \text{ \AA}$ of the W345 APOGEE-2 O-stars mentioned above. In the case of star #17 (2M02243615+6141161), it was not possible to extract a good blue-optical spectrum due to the low S/N in the blue spectral orders, which in turn is caused by high interstellar extinction. Fortunately, the red section region of its spectrum has higher S/N, with two helium spectral lines well suited for optical spectral type classification purposes.

He I and He II lines are clearly seen in the blue and red-optical spectra in Figure 4. The He II $\lambda 4542$ and the He I $\lambda 4471$ lines in the blue side, along with the He II $\lambda 5411$ and He I $\lambda 5876$ lines in the red side, are suitable for our spectral type classification purposes. Both line pairs yield EW ratios that correlate with the temperature sequence, in which the unit corresponds to the O7 spectral type (Walborn 1980). In Table 4,

Table 4
Line Parameters for the OB Star Candidates in the Blue-Red Optical Range

#	He λ 4471	He λ 4542	He λ 4922	He λ 5411	He λ 5876
20	0.40 (0.06)	0.74 (0.09)	0.08 (0.02)	1.41 (0.15)	0.69 (0.08)
17	1.06 (0.13)	1.21 (0.15)
46	0.88 (0.11)	0.55 (0.07)	0.43 (0.05)	0.83 (0.10)	0.93 (0.11)
21a	0.46 (0.06)	0.27 (0.03)	0.38 (0.05)	0.47 (0.06)	0.73 (0.09)
21b	0.21 (0.03)	...	0.18 (0.02)	0.05 (0.01)	0.22 (0.03)
26	1.28 (0.14)	...	0.69 (0.08)	...	0.67 (0.08)
13	0.47 (0.06)	1.07 (0.12)	0.07 (0.01)	1.52 (0.17)	0.68 (0.08)
25	0.79 (0.09)	...	1.47 (0.16)	0.25 (0.03)	0.88 (0.10)
3	1.12 (0.13)	0.39 (0.05)	0.63 (0.07)	0.75 (0.09)	0.84 (0.10)

Table 5
Blue to Red Optical Line Ratios and Spectral Type Classification for O Stars of the W345 APOGEE-2 Sample

#	[4471]/[4542] (blue)	[5876]/[5411] (red)	[SpT1] (blue)	[SpT2] (red)	He 4686 ^{a,b}	[SpT+Lum. class ^{b,c,d}] (Optical)	[SpT+Lum. class] (APOGEE-2)
20	0.54	0.49	O6	O5.5	...	O6 v z	O7.5 IV–V
17	...	1.14	...	O8.5	...	O8.5	O8 IV–V
46	1.6	1.12	O8.5	O7.5	Very Strong	O8 v	O8.5–O9 IV–V
21a	1.7	1.55	O8.5	O7.5	Strong	O8 III	O9–B0 III
21b	...	4.4	...	O9.5	...	O9.5	...
26	B-type	B-type	...	B0–B0.5 v	O9–B0 IV–V
13	0.44	0.45	O5.5	O5.5	...	O5.5 v z	O9.5 IV–V
25	2.9	3.52	O9.5	B0	...	O9.5–B0 v	O9–B0 IV–V
3	2.9	1.12	O9.5	O7.5	Very Strong	O8.5 v	O7.5 IV–V

Notes.

^a Strength of the He II 4686 line—Luminosity criteria for O8–O8.5 stars—Sota et al. (2011).

^b Accordingly with criteria in Table 4 of Sota et al. (2011).

^c Based on criteria from Tables 5 and 6 of Sota et al. (2011).

^d For B-stars, we used the criteria described in Walborn & Fitzpatrick (1990), Didelon (1982).

we list the measured EW values for these helium lines. In Table 5, we list the corresponding EW ratio values (4471/4542 and 5876/5411), together with the derived spectral types. These types were determined according to the canonical optical spectral classification procedure as defined by Conti & Alschuler (1971), Conti & Frost (1977), Mathys (1988), Walborn & Fitzpatrick (1990), and Sota et al. (2011).

The spectra in Figure 4 show that the He II λ 4686 lines of sources #13 and #20 are very strong, with the mentioned feature being the most intense helium line transition in both blue-optical spectrograms, which is known to be characteristic of the Vz class, as a signature of youth (Walborn et al. 2014). It seems that the Of effect (established as a luminosity indicator in normal O-type spectra) is suppressed by the Vz effect, generating less emission than seem in normal main-sequence spectra (Walborn et al. 2014). On the other hand, the He II λ 4686 line profiles from spectra #3 and #46 (both very strong), indicate that these two stars probably belong to luminosity class V (Sota et al. 2011). In the case of the O-star #17, the lack of a better quality blue-optical spectrum (containing the He II λ 4686 line) prevents an estimate of its luminosity class.

The next blue- and red-optical O-type spectra are those of star #21. A careful examination of its spectrograms reveals that all He I lines are double, indicating that the star is a binary system. In fact, the He II λ 4542 and He II λ 5411 lines of the primary are much stronger than those from the secondary (blueshifted). On the other hand, the He I λ 4471 and He I λ 5876 lines seem to be much stronger compared with the

associated He II λ 4542 and He II λ 5411 lines (blueshifted); therefore, a spectral type later than O9 is assigned for the secondary star. Based on the observed line intensities and ratios, and using the criteria defined by Sota et al. (2011), we concluded that source #21 is probably composed by O8 III and O9.5 III stars.

Finally, stars #25 and #26 have the latest spectral types in the sample. The relative intensities of C III λ 4650 and He II λ 4686 lines in their blue-optical spectra indicate that source #26 is probably a B0–B0.5 star (Sota et al. 2011), and a similar analysis for source #25 results in an spectral type ranging from O9.5–B0. From the criteria described by Didelon (1982), a luminosity class V is assigned for both stars. A summary of the optical features along with a comparison between APOGEE-2 and SPM spectral types is given in Table 5.

We notice that in a few cases, the spectral types derived based on the APOGEE spectra differ by more than one subtype from those found in the literature. From the 14 known O-stars present in the APOGEE-2 W345 sample, stars #1 (O6.5 + O8/B0), #10 (O5–O7 + O7–O9), #27 (O6 + O?), and #38 (O6.5 + O9–B0) are known to be binaries or, as in the case of star #27, a binary candidate. In such cases, APOGEE-2 spectral types seem to be biased toward the spectral type of the cooler companion, namely: (APOGEE-2 versus literature): #1 [O8.5–O9] versus [O6.5 + O8–B0], #10 [O8.5–O9] versus [O5–O7 + O7–O9], #27 [O6.5–O7] versus [O6 + O?], and #38 [O8.5] versus O6.5 + [O9–B0]. A possible explanation would be that the continuum of the later-type component would be

“veiling” (or dimming) the He II line in the combined spectrum. This, in turn, would produce a bias toward the cooler component. However, this assumption is based on a very small number of cases (three), and additional observations of a larger number of known binaries are necessary to confirm this hypothesis. Another possibility would be some veiling of the He II line produced by a significant flux contribution to the continuum in the H -band spectra, generated in the stellar wind and/or from some circumstellar material surrounding the star.

For the remaining 10 known O-stars (#2, 4, 6, 8, 12, 15, 16, 24, 32, 45), the agreement between the spectral types derived using APOGEE-2 spectra and those from the literature is good for eight of them (within one sub-type or better). The two cases in which our results do not match those from the literature are stars #12 and #24. In case of the former, we derived O6.5-O7 type, and from the literature it is assigned an O8.5 type, which is a difference of less than two sub-classes. On the other hand, star #24 is the earliest in the APOGEE-2 sample. From the APOGEE-2 spectrum, we derived a spectral type O6.5, which compared with the one derived from optical data (O4.5), is two sub-types later.

4. Summary and Future Work

In this work, we have applied the semi-empirical spectral classification method for massive stars described in Paper I to a sample of OB stars in the W345 complex. We classified 42 O-type stars in the W3/W4 regions and 18 in W5. Of these, 46 sources are previously unknown or mis-classified. The sources in our sample were selected as spectroscopy targets through NIR photometric selection criteria. Over 200 additional OB candidates not classified as O-type, are classified—with the same method—as B-type stars. The spectral types obtained with APOGEE-2 spectra were confirmed using optical spectra for nine stars in our sample. Therefore, we conclude that Br11 and Br13 lines together with He II 7–12 and He II 7–13 lines contained in the APOGEE-2 spectral range are useful in providing reliable spectral type classification down to one spectral sub-class, for massive stars in regions as distant as W345 ($d \sim 2$ kpc).

The large number of newly found O-type stars, as well as the numerous intermediate-mass B-type population, indicate that W345 is a very efficient massive star factory, with an integral stellar population probably amounting several thousand solar masses. We know from previous studies that the massive star population of W345 is contained in numerous clusters with evident substructure, so intermediate and massive stars in W345 play a crucial role for the evolution of this giant H II complex. In the case of OB stars, APOGEE-2 spectra have high enough resolution to provide radial velocity estimates with ~ 15 km s⁻¹ precision. This study, along with radial velocity estimates with precision of 1 km s⁻¹ or below for solar and sub-solar type stars observed in the same plates (C. Román-Zúñiga et al. 2019, in preparation), will allow for a detailed kinematic study of the complex, once we add distances and proper motions from GAIA DR2. These studies will be crucial to understanding large-scale expansion effects observed in young stellar population of the Perseus arm in the vicinity of W345 from proper motions (Román-Zúñiga et al. 2019). Also, special attention is being given to the B-type population observed in the same W345 APOGEE-2 plates (V. Ramirez-Preciado 2019, in preparation). As B-stars are intermediate-mass sources, and because O-type stars evolve rapidly and may be systematically

removed from clusters (Oh & Kroupa 2016; Román-Zúñiga et al. 2019; Wang et al. 2019), they probably play a key role in the structure and evolution of young clusters.

A.R.-L. acknowledges financial support provided in Chile by Comisión Nacional de Investigación Científica y Tecnológica (CONICYT) through the FONDECYT project 1170476 and by the QUIMAL project 130001, and support in Mexico from the PREI DGAPA UNAM program for academic exchange scholarship. C.R.-Z., M.T., J.H., and V.R.P. acknowledge support from UNAM-PAPIIT grants IN-108117, IN-104316, IA-103017. M.K. acknowledges support provided by the NSF through grant AST-1449476, and from the Research Corporation via a Time Domain Astrophysics Scialog award (#24217). G.S.S. was supported in part by NASA grant NNX13AF34G. D.M. is supported by the BASAL Center for Astro-physics and Associated Technologies (CATA) through grant AFB-170002, by the Ministry for the Economy, Development and Tourism, Programa Iniciativa Científica Milenio grant IC120009, awarded to the Millennium Institute of Astrophysics (MAS), and by FONDECYT No. 1170121. J.B. gratefully acknowledges support by the Ministry for the Economy, Development, and Tourism’s Millennium Science Initiative through grant IC 120009, awarded to the Millennium Institute of Astrophysics (MAS). D.A.G.H. and O.Z. acknowledge support provided by the Spanish Ministry of Economy and Competitiveness (MINECO) under grant AYA-2017-88254-P. We thank the staff of the Observatorio Astronómico Nacional in San Pedro Mártir for kind support during observations. Funding for the Sloan Digital Sky Survey IV has been provided by the Alfred P. Sloan Foundation, the U.S. Department of Energy Office of Science, and the Participating Institutions. SDSS-IV acknowledges support and resources from the Center for High-Performance Computing at the University of Utah. The SDSS website is www.sdss.org. SDSS-IV is managed by the Astrophysical Research Consortium for the Participating Institutions of the SDSS Collaboration including the Brazilian Participation Group, the Carnegie Institution for Science, Carnegie Mellon University, the Chilean Participation Group, the French Participation Group, Harvard-Smithsonian Center for Astrophysics, Instituto de Astrofísica de Canarias, The Johns Hopkins University, Kavli Institute for the Physics and Mathematics of the Universe (IPMU)/University of Tokyo, Lawrence Berkeley National Laboratory, Leibniz Institut für Astrophysik Potsdam (AIP), Max-Planck-Institut für Astronomie (MPIA Heidelberg), Max-Planck-Institut für Astrophysik (MPA Garching), Max-Planck-Institut für Extraterrestrische Physik (MPE), National Astronomical Observatories of China, New Mexico State University, New York University, University of Notre Dame, Observatório Nacional/MCTI, The Ohio State University, Pennsylvania State University, Shanghai Astronomical Observatory, United Kingdom Participation Group, Universidad Nacional Autónoma de México, University of Arizona, University of Colorado Boulder, University of Oxford, University of Portsmouth, University of Utah, University of Virginia, University of Washington, University of Wisconsin, Vanderbilt University, and Yale University. This research has made use of the SIMBAD database, operated at CDS, Strasbourg, France—Wenger et al. (2000). This research has made use of the VizieR catalog access tool, CDS, Strasbourg, France. The original description of the VizieR service was published in Ochsenbein et al. (2000). This publication makes

use of data products from the *Wide-field Infrared Survey Explorer*, which is a joint project of the University of California, Los Angeles, and the Jet Propulsion Laboratory/California Institute of Technology, funded by the National Aeronautics and Space Administration.

Facilities: Sloan Telescope, APOGEE, OANSPM:2.1 m.
Software: IRAF.

ORCID iDs


Alexandre Roman-Lopes  <https://orcid.org/0000-0002-1379-4204>

Carlos G. Román-Zúñiga  <https://orcid.org/0000-0001-8600-4798>

Mauricio Tapia  <https://orcid.org/0000-0002-0506-9854>

Valeria Ramírez-Preciado  <https://orcid.org/0000-0002-4013-2716>

Guy S. Stringfellow  <https://orcid.org/0000-0003-1479-3059>

Jason E. Ybarra  <https://orcid.org/0000-0002-3576-4508>

Jinyoung Serena Kim  <https://orcid.org/0000-0001-6072-9344>

Dante Minniti  <https://orcid.org/0000-0002-7064-099X>

Kevin R. Covey  <https://orcid.org/0000-0001-6914-7797>

Marina Kounkel  <https://orcid.org/0000-0002-5365-1267>

Genaro Suárez  <https://orcid.org/0000-0002-2011-4924>

Jura Borissova  <https://orcid.org/0000-0002-5936-7718>

D. A. García-Hernández  <https://orcid.org/0000-0002-1693-2721>

References

- Abt, H. A., & Corbally, C. J. 2000, *ApJ*, 541, 841
- Basu, S., Johnstone, D., & Martin, P. G. 1999, *ApJ*, 516, 843
- Bik, A., Henning, Th., Stolte, A., et al. 2012, *ApJ*, 744, 87
- Blanton, M. R., Bershady, M. A., Abolfathi, B., et al. 2017, *AJ*, 154, 28
- Carpenter, J. M., Heyer, M. H., & Snell, R. L. 2000, *ApJS*, 130, 381
- Chavarría, L., Allen, L., Brunt, C., et al. 2014, *MNRAS*, 439, 3719
- Cohen, M., & Lewis, R. R. 1978, *MNRAS*, 184, 801
- Conti, P. S., & Alschuler, W. R. 1971, *ApJ*, 170, 325
- Conti, P. S., & Frost, S. A. 1977, *ApJ*, 212, 728
- Cottaar, M., Covey, K. R., Foster, J. B., et al. 2015, *ApJ*, 807, 27
- Da Rio, N., Tan, J. C., Covey, K. R., et al. 2016, *ApJ*, 818, 59
- De Becker, M., Rauw, G., Manfroid, J., & Eenens, P. 2006, *A&A*, 456, 1121
- Deharveng, L., Zavagno, A., Anderson, L. D., et al. 2012, *A&A*, 546, A74
- Didelon, P. 1982, *A&AS*, 50, 199
- Eisenstein, D. J., Weinberg, D. H., Agol, E., et al. 2011, *AJ*, 142, 72
- Foster, J. B., Cottaar, M., Covey, K. R., et al. 2015, *ApJ*, 799, 136
- Gao, X. Y., Reich, W., Reich, P., Han, J. L., & Kothes, R. 2015, *A&A*, 578, A24
- Gunn, J. E., Siegmund, W. A., Mannery, E. J., et al. 2006, *AJ*, 131, 2332
- Hachisuka, K., Brunthaler, A., Menten, K. M., et al. 2006, *ApJ*, 645, 337
- Hardorp, J., Rohlf, K., Slettebak, A., & Stock, J. 1959, *LS*, C01
- Hiltner, W. A. 1956, *ApJS*, 2, 389
- Jose, J., Kim, J. S., Herczeg, G. J., et al. 2016, *ApJ*, 822, 49
- Karr, J. L., & Martin, P. G. 2003, *ApJ*, 595, 900
- Kiminki, M. M., Kim, J. S., Bagley, M. B., Sherry, W. H., & Rieke, G. H. 2015, *ApJ*, 813, 42
- Koenig, X. P., Allen, L. E., Gutermuth, R. A., et al. 2008, *ApJ*, 688, 1142
- Kounkel, M., Covey, K., Suárez, G., et al. 2018, *AJ*, 156, 84
- Maíz Apellániz, J., Sota, A., Arias, J. I., et al. 2016, *ApJS*, 224, 4
- Majewski, S. R., Schiavon, R. P., Frinchaboy, P. M., et al. 2017, *AJ*, 154, 94
- Massey, P., Johnson, K. E., & Degioia-Eastwood, K. 1995, *ApJ*, 454, 151
- Mathys, G. 1988, *A&AS*, 76, 427
- Mathys, G. 1989, *A&AS*, 81, 237
- Navarete, F., Figueredo, E., Damineli, A., et al. 2011, *AJ*, 142, 67
- Nidever, D. L., Holtzman, J. A., Allende Prieto, C., et al. 2015, *AJ*, 150, 173
- Niwa, T., Tachihara, K., Itoh, Y., et al. 2009, *A&A*, 500, 1119
- Ochsenbein, F., Bauer, P., & Marcout, J. 2000, *A&AS*, 143, 23
- Oey, M. S., Watson, A. M., Kern, K., & Walth, G. L. 2005, *AJ*, 129, 393
- Oh, S., & Kroupa, P. 2016, *A&A*, 590, A107
- Panwar, N., Samal, M. R., Pandey, A. K., et al. 2017, *MNRAS*, 468, 2684
- Rauw, G., & De Becker, M. 2004, *A&A*, 421, 693
- Rauw, G., & Nazé, Y. 2016, *A&A*, 594, A82
- Rivera-Ingraham, A., Martin, P. G., Polychroni, D., et al. 2013, *ApJ*, 766, 85
- Rivera-Ingraham, A., Martin, P. G., Polychroni, D., et al. 2015, *ApJ*, 809, 81
- Rivera-Ingraham, A., Martin, P. G., Polychroni, D., & Moore, T. J. T. 2011, *ApJ*, 743, 39
- Roman-Lopes, A., Franco, G. A. P., & Sanmartin, D. 2016, *ApJ*, 823, 96
- Roman-Lopes, A., Román-Zúñiga, C., Tapia, M., et al. 2018, *ApJ*, 855, 68
- Román-Zúñiga, C., Roman-Lopes, A., Tapia, M., Hernández, J., & Ramírez-Preciado, V. 2019, *ApJ*, 871, 12
- Román-Zúñiga, C. G., Ybarra, J. E., Megías, G. D., et al. 2015, *AJ*, 150, 80
- Rydstrom, B. A. 1978, *A&AS*, 32, 25
- Shi, H. M., & Hu, J. Y. 1999, *A&AS*, 136, 313
- Skrutskie, M. F., Cutri, R. M., Stiening, R., et al. 2006, *AJ*, 131, 1163
- Sota, A., Maíz Apellániz, J., Morrell, N. I., et al. 2014, *ApJS*, 211, 10
- Sota, A., Maíz Apellániz, J., Walborn, N. R., et al. 2011, *ApJ*, 193, 24
- Straizys, V., Boyle, R. P., Janusz, R., et al. 2013, *A&A*, 554, A3
- Sung, H., Bessell, M. S., Chun, M.-Y., et al. 2017, *ApJS*, 230, 3
- Thronson, H. A., Jr., Lada, C. J., & Hewagama, T. 1985, *ApJ*, 297, 662
- Voroshilov, V. I., Guseva, N. G., Kalandadze, N. B., et al. 1985, Catalog of BV magnitudes and spectral classes of 6000 stars
- Walborn, N. R. 1980, *ApJS*, 44, 535
- Walborn, N. R., & Fitzpatrick, E. L. 1990, *PASP*, 102, 379
- Walborn, N. R., Sana, H., Simón-Díaz, S., et al. 2014, *A&A*, 564, 40
- Wang, L., Kroupa, P., & Jerabkova, T. 2019, *MNRAS*, 484, 1843
- Wenger, M., Ochsenbein, F., Egret, D., et al. 2000, *A&AS*, 143, 9
- Wilson, J. C., Hearty, F., Skrutskie, M. F., et al. 2010, *Proc. SPIE*, 7735, 77351
- Wood, D. O. S., & Churchwell, E. d. 1989, *ApJ*, 340, 265
- Zasowski, G., Cohen, R. E., Chojnowski, S. D., et al. 2017, *AJ*, 154, 198